(12)

AD A115367

OPTICAL EXCISION PROGRAM
OPTICAL EXCISOR FIELD TESTS

PSI-ER-5538-04

PROBE SYSTEMS, INCORPORATED
655 NORTH PASTORIA AVENUE
SUNNYVALE, CALIFORNIA

OPTICAL EXCISION PROGRAM

OPTICAL EXCISOR FIELD TESTS

PSI-ER-5538-04

February 1982

ARPA Order Number: 3621
Program Code Number: 8E20
Effective Date of Contract: 28 December 1978
Contract Expiration Date: 28 February 1982
Contract Number: N00039-79-C-0141
Principal Investigator: Dave Jackson, (408) 732-6550

DARPA NAVELEX JOINT PROGRAM
Sponsored By
Defense Advanced Research Projects Agency
ARPA Order No. 3621
Sponsored and Monitored By
NAVELEX Under Contract No. N00039-79-C-0141

The views and conclusions contained in this document are those of the authors and should not be interpreted as representing the official policies, either expressed or implied, of the Defense Advanced Research Projects Agency or the U.S. Government.

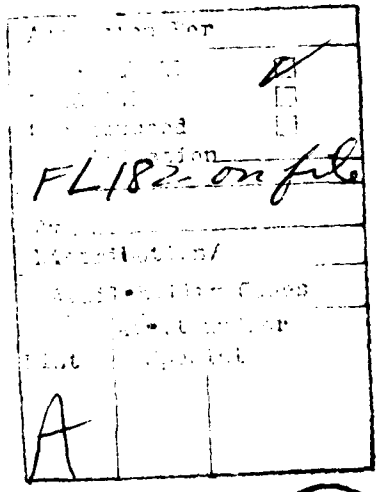

TABLE OF CONTENTS

LIST OF ILLUSTRATIONS

LIST OF TABLES

EXECUTIVE SUMMARY

A brassboard optical excisor was tested in a real-world spread spectrum intercept system with both actual and simulated signals. It was shown that the vulnerability of the spread spectrum intercept system to narrowband jammer interference was significantly reduced by the frequency selective rejection capabilities of the optical excisor.

The brassboard optical excisor was assembled on a 2 x 4 foot table and had 40 megahertz of coherent bandwidth with approximately 200 resolvable frequencies. This brassboard was tested inside a van which contains 3 full racks of equipment devoted to spread spectrum intercept.

Test data for a spread spectrum chip detector with and without an optical excisor were collected. This data utilized a simulated spread spectrum signal having a 10 megahertz chip rate and a negative signal-to-noise ratio combined with a simulated narrowband jammer. With optical excision, the chip detector demonstrated a 25 dB improvement in narrowband jammer noise immunity with essentially no degradation in chip detector sensitivity when compared to the chip detector without optical excision. These tests also demonstrated the optical excisor's ability to coherently process broadband signals while achieving a frequency stability better than 3.3 hertz.

Test data for a switched (Dicke) radiometer was also collected with and without an optical excisor. A real-world push-to-talk narrowband interference signal was utilized in these experiments in addition to the simulated spread spectrum and narrowband jammer signals. The optical excisor was used to eliminate the effects of the narrowband jammers on the radiometer output.

SECTION 1.0
INTRODUCTION

This special technical report describes the results of a task conducted by PROBE SYSTEMS as part of the DARPA/NAVELEX Joint Program for Optical Excision. The objective of this task was to demonstrate the optical excisor operating as a part of an intercept system in an environment as realistic as possible. Data was collected allowing comparison of system performance with and without optical excision of interference. This work resulted in the successful demonstration of the optical excisor and provides confidence that it is operable with real-world receiver systems and in operational environments.

Optical excision is a signal processing technique for eliminating narrowband RF interference signals. This technique uses an acousto-optical Bragg cell and a continuous laser to spatially form the signal spectrum of an electrical input. By blocking narrowband interference in the optically-generated signal spectrum and coherently detecting the remainder of the spectrum, an interference-free broadband RF signal is obtained as the output of the processor.

The field tests employed the brassboard model optical excisor developed by PROBE SYSTEMS under the Optical Excision Program and the Teal Wing intercept system. These are described in appendices A and B respectively. Section 2 describes the testing conducted by PROBE and section 3 presents the test data obtained. Conclusions made as a result of these tests are the subject of section 4.

SECTION 2.0
TEST DESCRIPTION

2.1 INTRODUCTION

Two signal processors are examined in this test program. They are the switched or Dicke radiometer and the chip rate detector. The performance of each processor was determined with and without optical excision of a narrowband CW jammer.

2.2 CHIP DETECTOR

Figure 2-1 shows the test configuration for the chip detector.

The test signal generator was used to generate a BPSK modulated PN spread spectrum signal with a chipping rate of 10 MHz centered at 362.3 MHz and with a null to null BW of 20 MHz. The wavetek was used to simulate a CW jammer and was set at 365.3 MHz. The signal level of the test generator was controlled by a variable Hewlett Packard attenuator and the wavetek level was set by an attenuator on its control panel. The two signals are then power combined passed through another variable attenuator and then power divided.

The primary IF channel IF2 feeds the detector and the secondary channel IF1 feeds the HP spectrum analyzer. The signal is monitored at this point to check for the presence or absence of the jammer and also to check for IF amplifier saturation.

The primary IF channel IF2 was set to a bandwidth of 35 megahertz centered at 362.5 megahertz. This 35 megahertz IF bandwidth was slightly less than the 40 megahertz bandwidth of the brassboard optical excisor. IF channel IF1 was set to a bandwidth of 120 megahertz centered at 362.5 megahertz. This wider bandwidth for the IF1 channel ensured a flat magnitude response for monitoring the signals of interest with the HP spectrum analyzer. Both of the

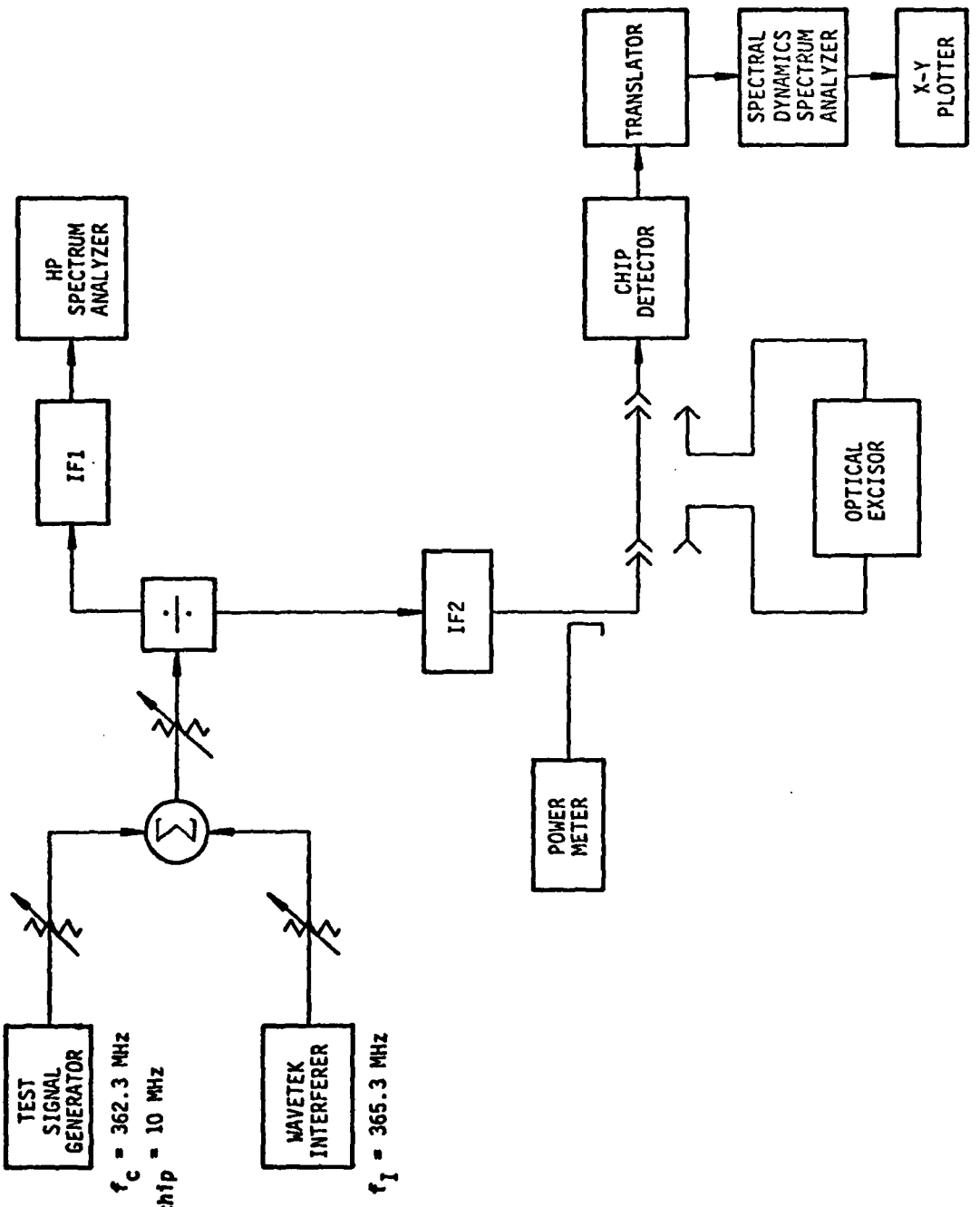

FIGURE 2-1 SENSITIVITY TEST BLOCK DIAGRAM

filters in the IF1 and IF2 channels are followed by low noise amplifiers to set the system noise figure.

The primary IF amp either feeds the chip detector through an electrical short or feeds the optical processor. Except for the removal of the jammer the optical signal processor is set to as near unity gain as possible to emulate a short circuit and avoid overdriving the chip detector.

The chip detector multiplies the signal by a delayed version of itself and then presents a feature line to the frequency translator which passes the feature line off to the spectrum analyzer. The spectrum analyzer was set to an integration time window of 0.3 seconds to obtain a frequency resolution of 3.3 hertz. The resultant signal and noise power spectrums from 8 such windows were averaged to obtain the power spectrum for recording on the output X, Y plotter.

To measure the sensitivity the following procedure was used. First the Ø dB SNR was found for both the spread signal (SNR = S/N) and the narrowband jammer (SNR = J/N) by attenuating both the signal and jammer and measuring the noise floor in dBm with the power meter. The signal or jammer level but not both is then increased until the power meter reads 3 dB above the noise floor. This level of attenuation is then noted and any attenuation more or less is considered the negative or positive signal to noise ratio, respectively.

The sensitivity is defined as the input spread signal to noise ratio (S/N) to the detector that ensures a 10 dB signal to noise ratio at the output of the detector. The output 10 dB SNR was measured on a spectral dynamics spectrum analyzer and was measured as the difference between the peak of the feature line and the average noise floor level. To help in establishing a median noise value 8 averages of the feature in noise were taken by the spectrum analyzer itself. The final data was taken in permanent form on annotated X-Y plots.

2.3 SWITCHED RADIOMETER

The initial switched radiometer test configuration is given in Figure 2-2. The jammer in the form of a CW signal from the wavetek and the spread spectrum signal from the test signal generator are power combined. Each of the jammer and signal are separately controlled via attenuators and the jammer-signal combination is also controlled by a variable attenuator.

The signal plus jammer then enters an RF switch and the output of that switch is toggled between the signal plus jammer and the stable noise source. The switched signal is then bandpass filtered to remove any switching transients. The signal is then power divided to IF1 for observation and IF2 for detection. As before, IF2 is set to a bandwidth of 35 MHz entered at 362.5 MHz while IF1 is set to a bandwidth of 120 MHz centered at 336.5 MHz. The power meter is used to check levels during the test and its setup. The radiometer's output is permanently recorded on the strip chart recorder. The 0 dB signal and jammer levels were found as before. That is the noise floor was measured and signal or noise added (but not both) until a 3 dB increase in the noise floor was noted. The respective attenuator settings that accomplished this were noted and used as a 0 dB reference. The optical excision equipment was set to 0 dB gain and the strip chart recorder was calibrated.

A switched radiometer integrates the difference in signal energies between its reference noise source and the external signal over the bandwidth of detector for the integration time selected.

The first group of data collected was for the test signal generator and the wavetek simulating a jammer. Next we used an intermittent jammer from a presumed push to talk communication system as received by an antenna mounted on the roof of PROBE SYSTEMS. The center frequency of this "real world" interferer was determined using the configuration shown in Figure 2-3. The filtered antenna input is power combined with the wavetek, fed through the IF2 channel and displayed on the HP spectrum analyzer. The wavetek was adjusted in frequency until the wavetek's signal was as nearly as possible superimposed on

the intermittent push-to-talk interferer. The frequency thus determined was found to be 357.6 MHz.

The circuit was then reconnected so the real world interferer could be run in place of the wavetek as an intended jammer. See Figure 2-4. This last test was run to demonstrate the effectiveness of optical excision against a known actual interferer.

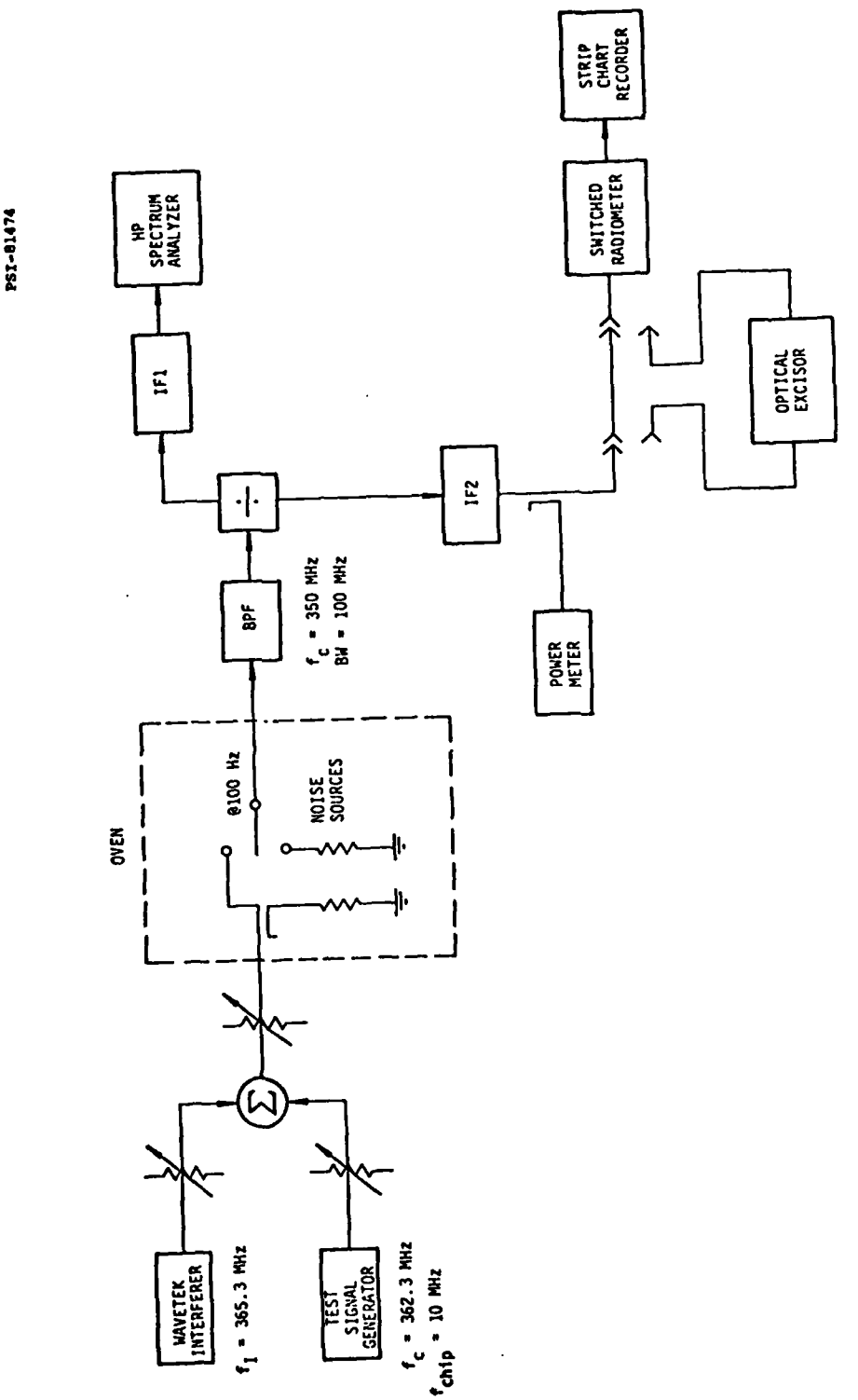

FIGURE 2-2 SWITCHED RADIOMETER TESTS

0122A

PSI-81472

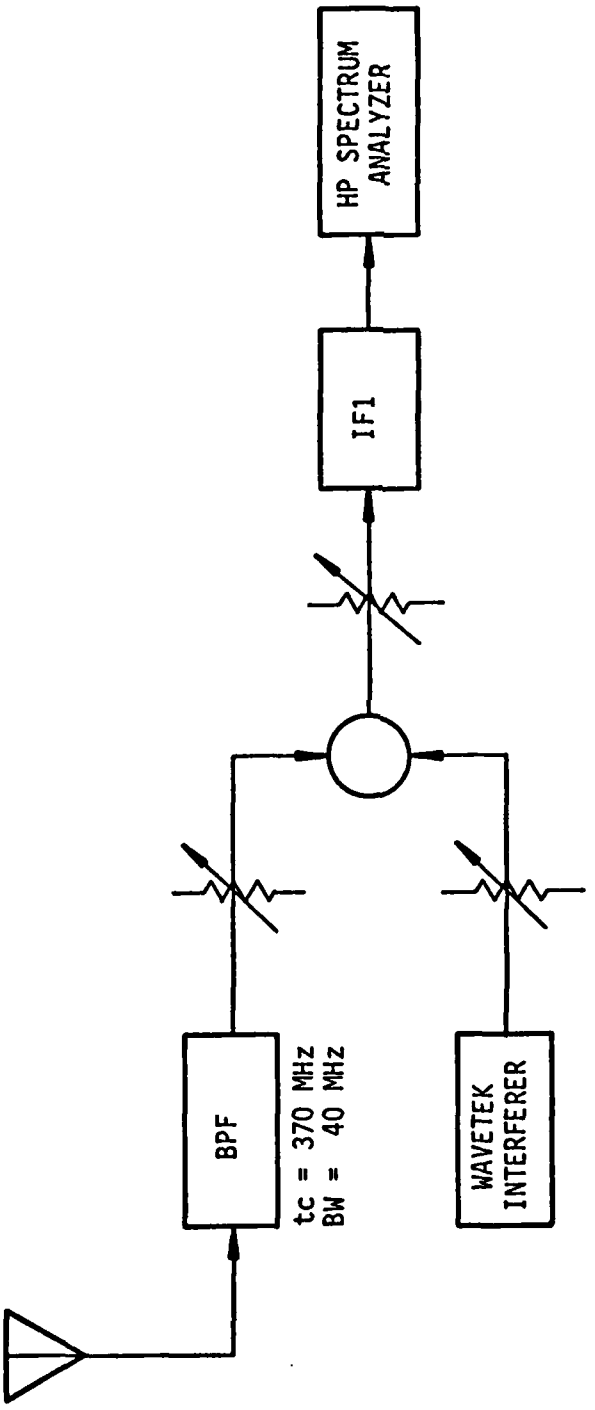

FIGURE 2-3 JAMMER CENTER FREQUENCY DETERMINATION

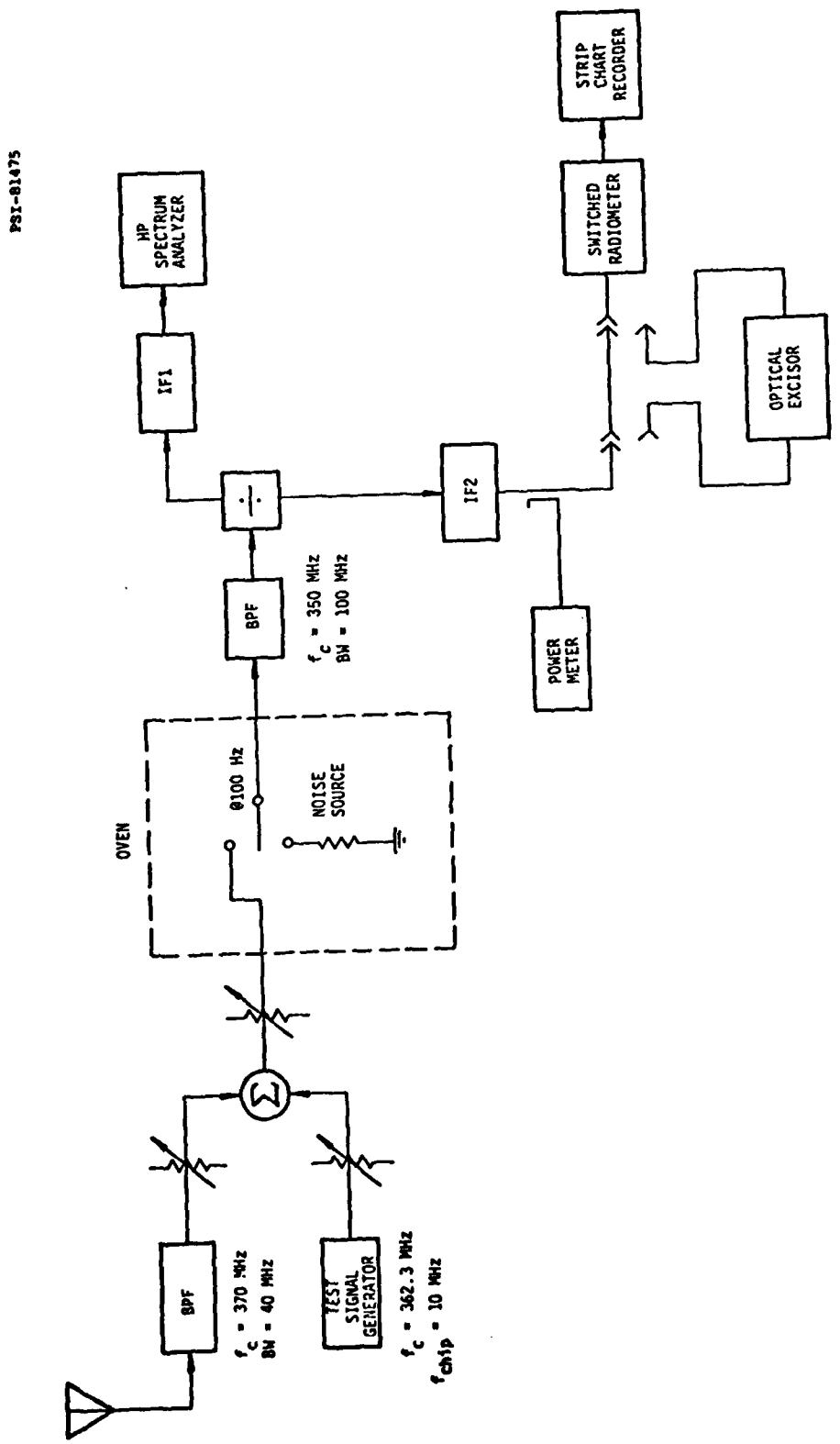

FIGURE 2-4 REAL WORLD EXCISION

3.0 TEST DATA

3.1 INTRODUCTION

The test data for each detector is described below. The chip detector data are presented first in section 3.2 while the switched radiometer data are presented in section 3.3.

3.2 CHIP DETECTOR DATA

The field test data for the chip detector sensitivity performance with and without optical excision of a jammer is given in tabular and graphical terms in Figures 3-1 and 3-2 respectively. Also included is the theoretical performance loss of a detector as derived in Appendix C.

Notice that the loss in sensitivity of the chip detector without optical excision in the presence of a jammer is never more than 2 dB worse than the theoretical loss and that as the J/N ratio decreases the actual data asymtotically approaches the theoretical curve.

In marked contrast to the nonexcised case, the sensitivity of the chip detector with the jammer excised is practically independent of the J/N ratio up to a J/N of 20 dB. The price paid in sensitivity over the jammer free case is approximately 1 dB. In fact the performance of the detector with excision is superior to the chip detector without excision for J/N ratios as low as -5 dB. Thus the optical excisor improves the narrowband jammer noise immunity of the chip detector by 25 dB over the nonexcised case.

The fact that the optical excisor did not significantly reduce the sensitivity of the chip detector implies that the optical excisor can coherently process signals with little or no phase distortion. Additionally, the fine frequency resolution of 3.3 hertz used for detecting the chip feature line demonstrated that the optical excisor frequency stability exceeded 3.3 hertz.

Jammer SNR J/N, dB	NO EXCISION			OPTICAL EXCISION	
	Measured Sensitivity S/N, dB	Measured Degradation dB	Theoretical* Degradation D_i, dB	Measured Sensitivity S/N, dB	Measured Degradation db
$-\infty$	-27.	0	0	-27	0
-20	-26.5	- .5	- .043	-26	-1
-15	-26.	- 1		-26	-1
-10	-26	- 1	- .4	-26	-1
- 5	-25	- 2		-26	-1
0	-24	- 3	- 2.35	-26	-1
5	-21.5	- 5.5	- 4.35	-26	-1
10	-18	- 9	- 6.6	-26	-1
15	-16	-11	- 9.0	-26	-1
20	-13	-14	-11.5	-26	-1
Plot Symbol		△	⊙		⊡

*The theoretical degradation D_i of the input sensitivity is equal to the square root of the theoretical degradation of the output sensitivity. From Appendix C, this yields $D_i = D^{\frac{1}{2}} = [1/(1 + 2J/N)]^{\frac{1}{2}}$.

FIGURE 3-1 CHIP DETECTOR SENSITIVITIES

PSI-81475

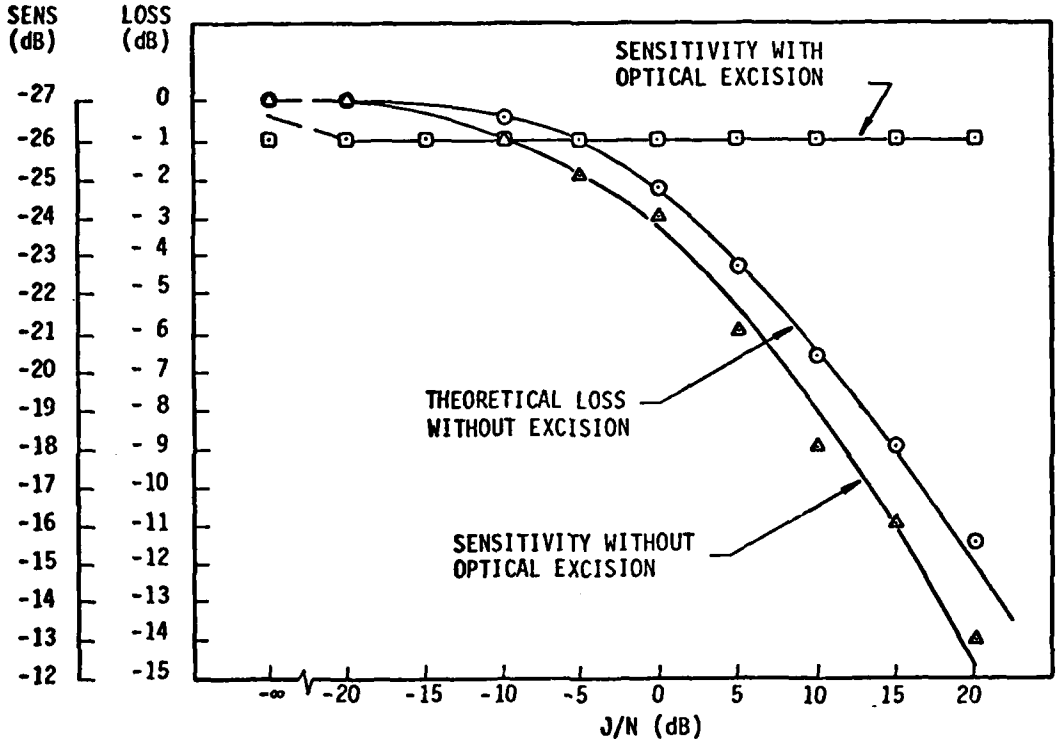

FIGURE 3-2 CHIP DETECTOR SENSITIVITY PERFORMANCE

3.3 SWITCHED RADIOMETER DATA

The switched radiometer output for the test configuration using the wavetek as a jammer (recall Figure 2-2) is given in Figures 3-3 and 3-4. These plots show the radiometer output versus time where time increases going from right to left. Figure 3-4 is a continuation of Figure 3-3. Changes in the spread signal to noise power S/N and jammer to noise power J/N are indicated.

Note that the noise floor at the beginning of the run in Figure 3-3 and at its termination is the same level. Also note in Figure 3-3 that when the J/N ratio increases from -00 to -20 dB there is virtually no increase in detected energy. However, the change of the J/N from -20 dB to -10 dB does shown an energy increase and a wide fluctuation. This is interpreted to be due to some of the light slipping past the excising wire due to thermal changes and/or vibrations. In later data where more care was taken this effect is not evident.

Finally note the dramatic rise in detected signal and jammer energy when the jammer is no longer excised (see Figure 3-3), and the equally dramatic change when the jammer is turned off (i.e., S/N = -20 dB and J/N = -20 in Figure 3-3). These last two examples show how effective the excision process is.

The second two strip chart recordings (Figures 3-4 and 3-5) show the switched radiometers response to the presence of a real world push to talk interferer. Figure 3-4 shows the radiometer detection without excision while Figure 3-5 shows the ability of the optical excisor to remove a jammer of negative (i.e., -14 dB) jammer to noise ratio. Note that the black bars along the baseline of the graph indicate the presence of the interferer.

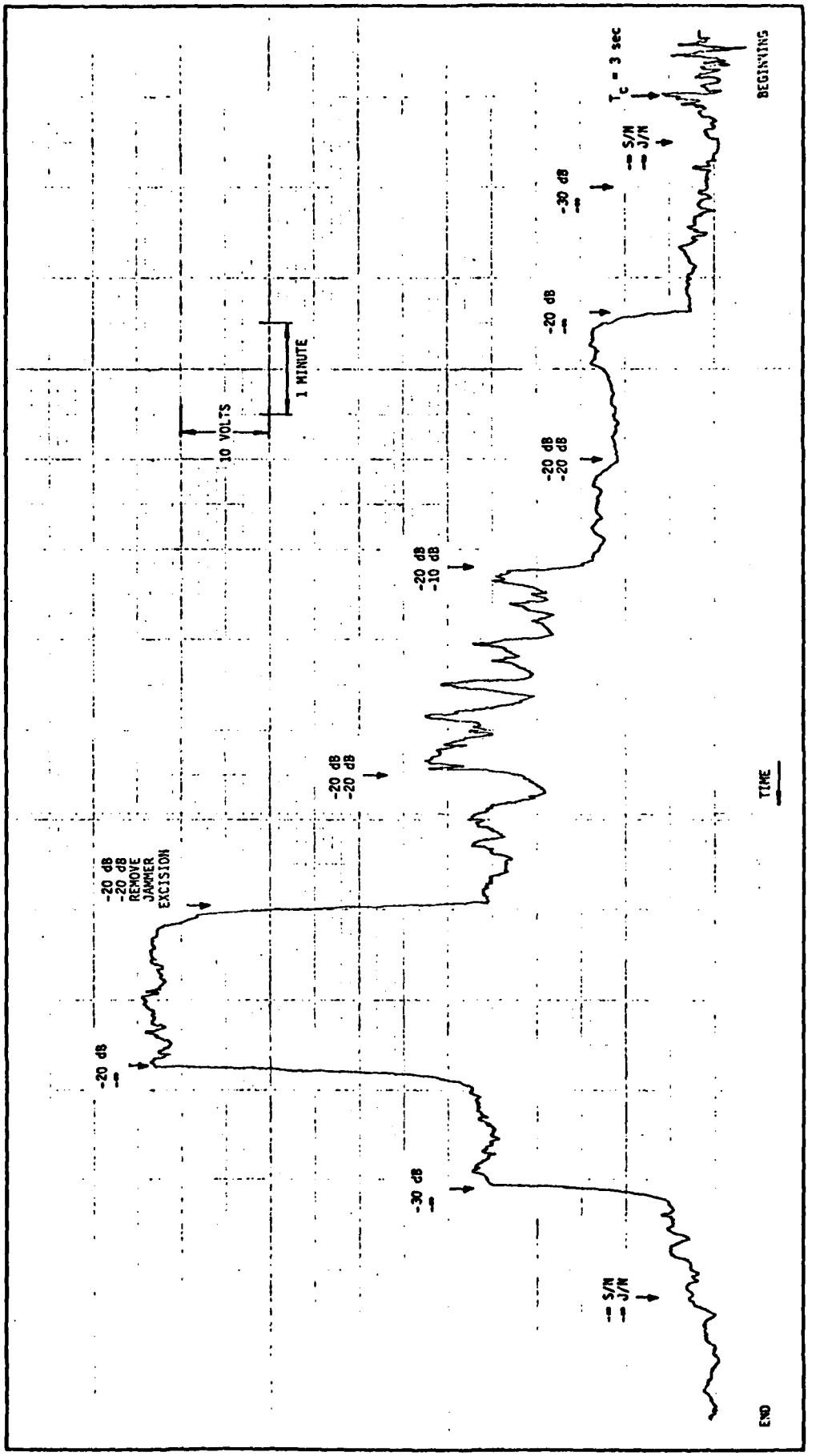

FIGURE 3-3 SWITCHED RADIOMETER DATA

0122A

PSI-80126

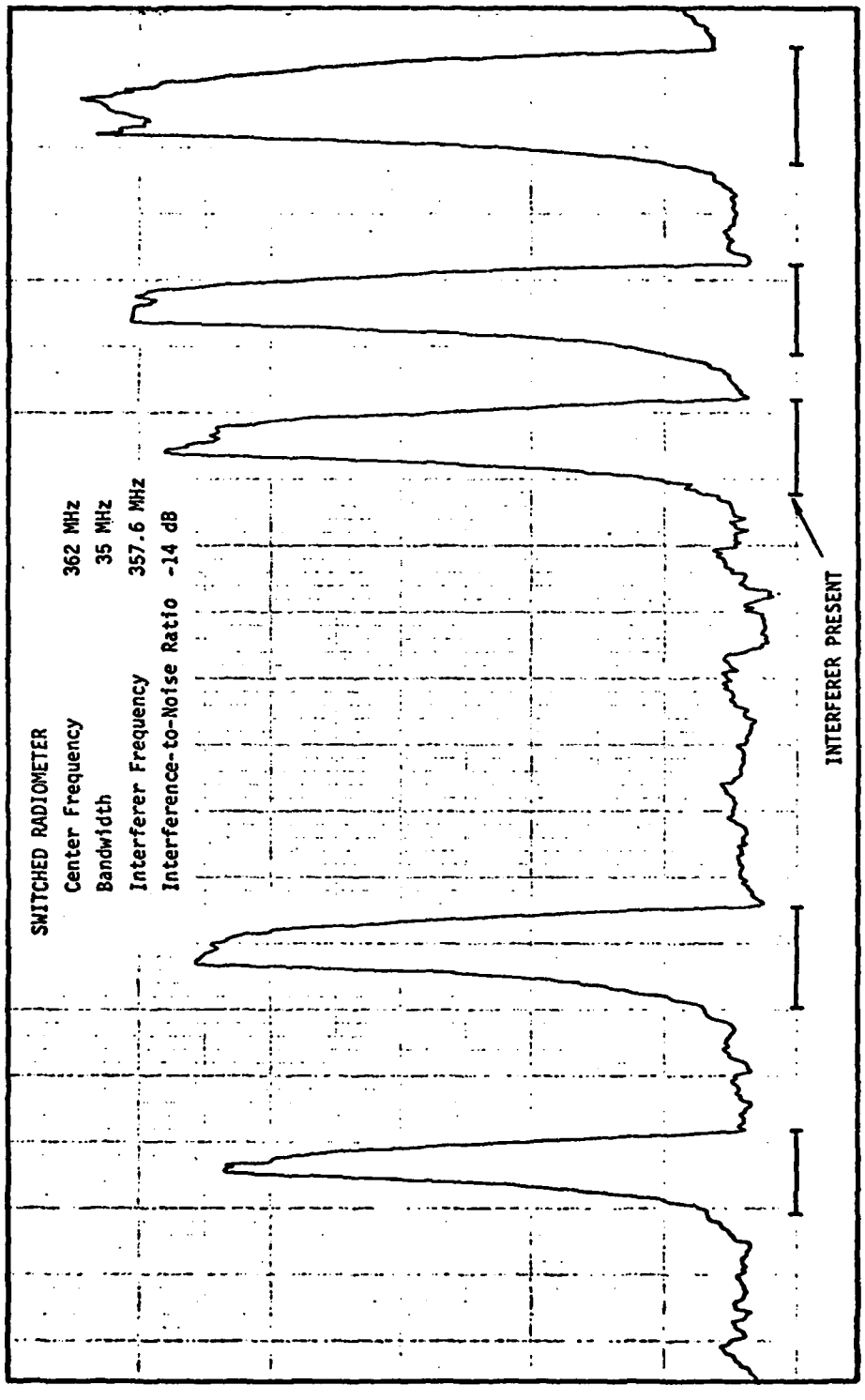

FIGURE 3-4 FIELD TESTS - WITHOUT EXCISOR

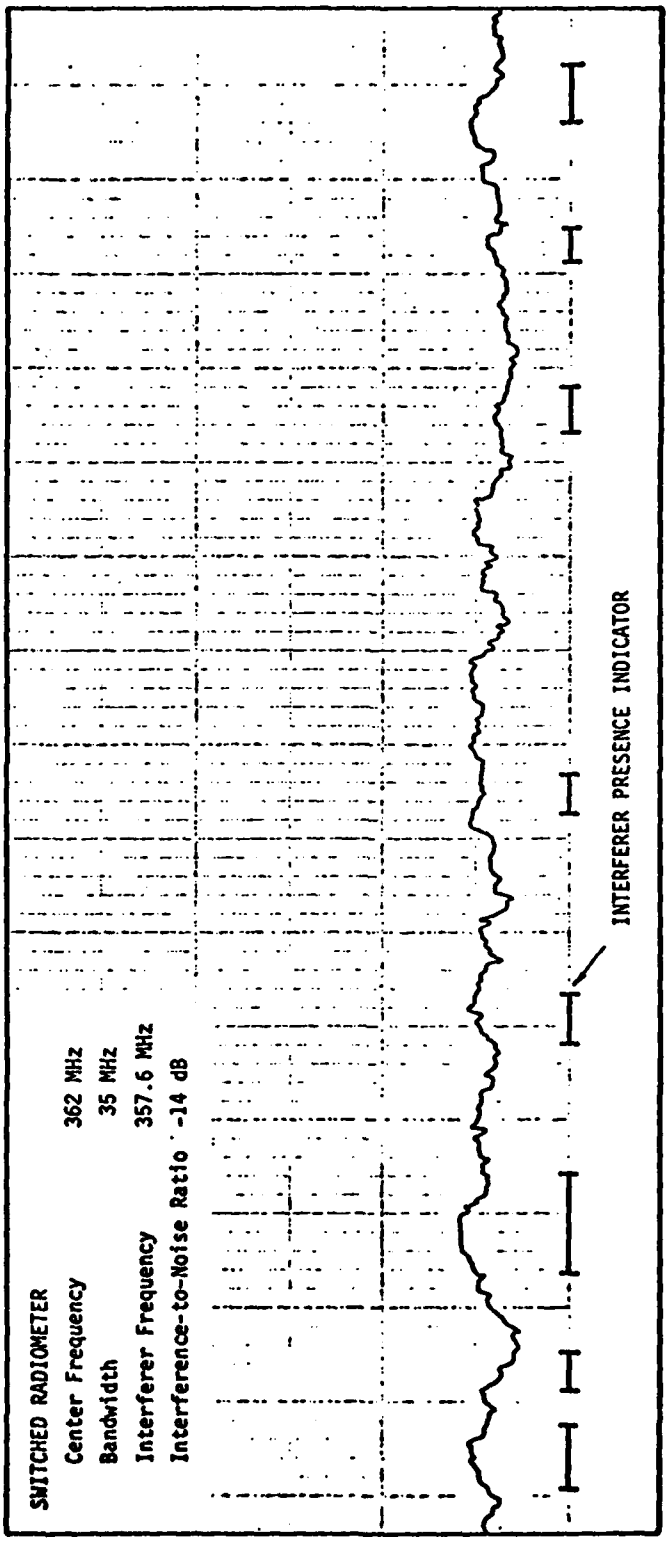

FIGURE 3-5 FIELD TEST - WITH EXCISOR

SECTION 4.0
CONCLUSIONS

The brassboard optical excisor was operated with a real-world spread spectrum intercept system with both actual and simulated signals. The vulnerability of the spread spectrum intercept system to narrowband jammer interference was significantly reduced by the frequency selective rejection capabilities of the optical excisor.

With optical excision, the spread spectrum chip detector demonstrated a 25 dB improvement in narrowband jammer noise immunity with essentially no degradation in the chip detector sensitivity. The data also demonstrated the optical excisor's ability to coherently process broadband signals while achieving a frequency stability better than 3.3 hertz. The utility of the optical excisor for total power radiometers such as the switched (Dicke) radiometer was also demonstrated.

APPENDIX A
BRASSBOARD OPTICAL EXCISOR

A part of the DARPA/NAVELEX Joint Program for Optical Excision included development of an engineering brassboard model optical excisor. The objective of this effort was to demonstrate the first level reduction in size of the laboratory model excisor allowing it to be tested and used in other than a laboratory environment. The brassboard model was designed, built, and tested by PROBE SYSTEMS and its description is the subject of this appendix.

At the conclusion of the laboratory testing of the optical excisor an optimum configuration for the brassboard model was specified. Many of the components to be used were already acquired in the first phase of the contract; the only exceptions were lenses of a shorter focal length and a small optical table.

Figure A-1 shows the optical layout for the brassboard. This optical layout was configured on a 2 x 4 foot honeycomb board. A 5 mw argon ion laser was used to generate an optical beam at a wavelength of 514.5 nm. After folding the beam, a short focal length cylindrical and a 26" focal length spherical achromat lens were used to obtain the Gaussian sheet beam illuminating the Bragg cell. Once through the cell, the diffracted signal spectrum was brought into focus at the Fourier transform plane by the 26" focal length transform lens. A hologram was placed in the path just past the transform lens to derive a reference beam from the DC or undiffracted optical beam. This holographic LO acts as a partial negative lens, i.e., only part of the light passing through it is diffracted. The result of this is that the signal spectrum falling on the photomultiplier is fully illuminated by undiffracted light from the Bragg cell which acts as the local oscillator for the photo mixing that occurs on the photocathode. (A thorough description of the holographic LO may be found in PSI-ER-5538-01.) Excision of signals was performed by placing a fine wire (AWG No. 40) at the transform plane and blocking the spectrum component to be excised.

PSI-81471

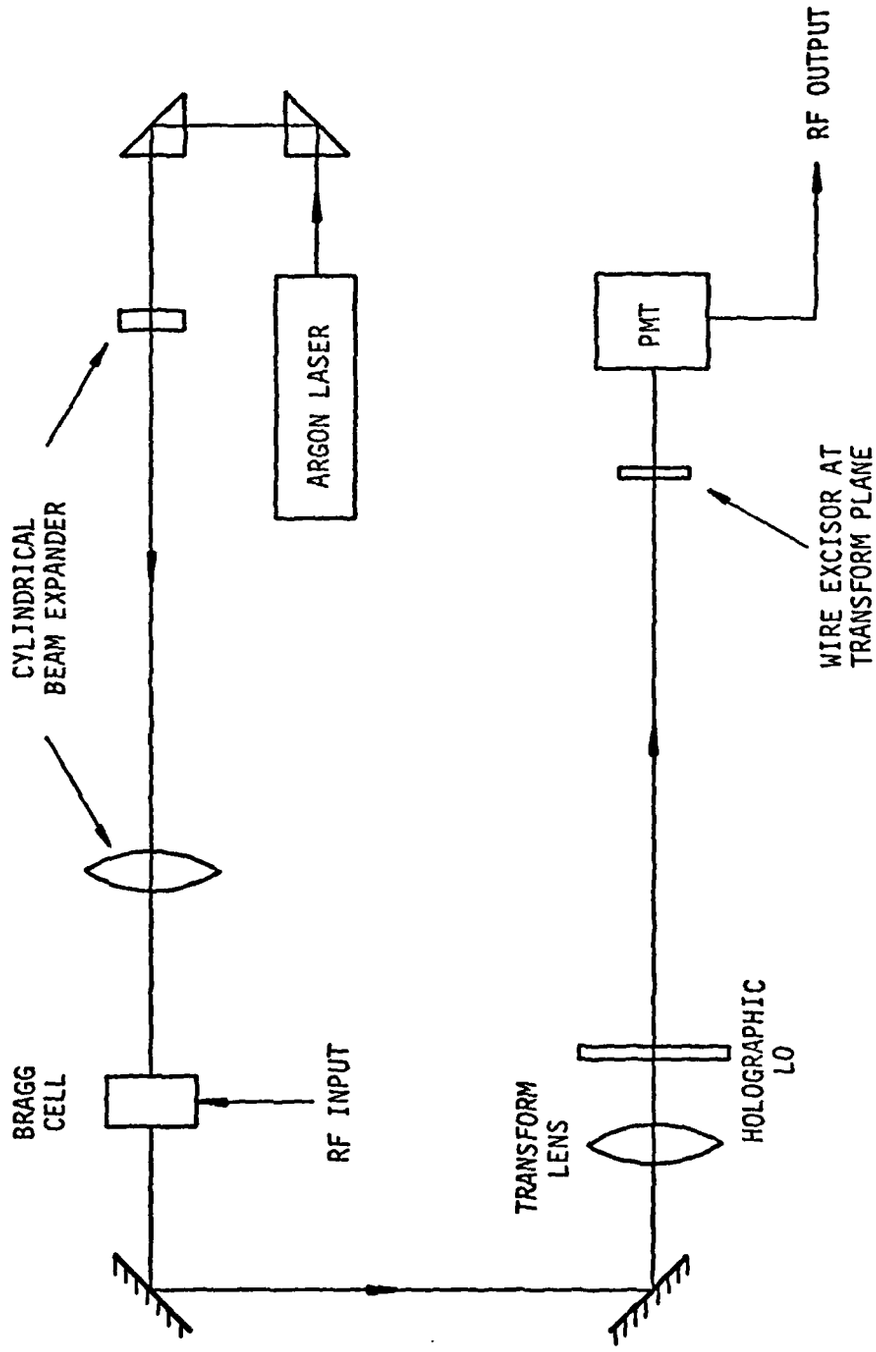

FIGURE A-1 BRASSBOARD OPTICAL SIGNAL EXCISOR

Figure A-2 shows a block diagram of the electronics directly associated with the optical signal excisor. Signals from the Teal Wing IF output are first downconverted to the Bragg cell center frequency of 70 MHz. This signal is bandpass filtered after passing through a step attenuator, resulting in a 40 MHz bandwidth passband. A power amplifier then amplifies the signal to a level appropriate for driving the Bragg cell in the optical processor.

The signal spectrum is coherently detected in the optical processor by a wide bandwidth, large active area photomultiplier tube. At this point the tube output is a low level signal and is fed to a low noise, high gain front end amplifier in the excisor electronics. After attenuation and again bandpass filtering the signal is further amplified and then up converted to the same center frequency that the Teal Wing IF output had.

By proper setting of the attenuators in the excisor electronics, power levels and the SNR could be controlled making the optical excisor appear to be a short circuit except that the excised interference is reduced in amplitude by as much as 35 dB.

A photograph of the brassboard optical excisor in operation inside the Teal Wing van is shown in Figure A-3. Located directly below the 2 x 4 foot brassboard are the laser power supply, the photomultiplier tube power supply, the signal conditioning electronics and the wavetek signal generator used for the local oscillator of the signal conditioning electronics.

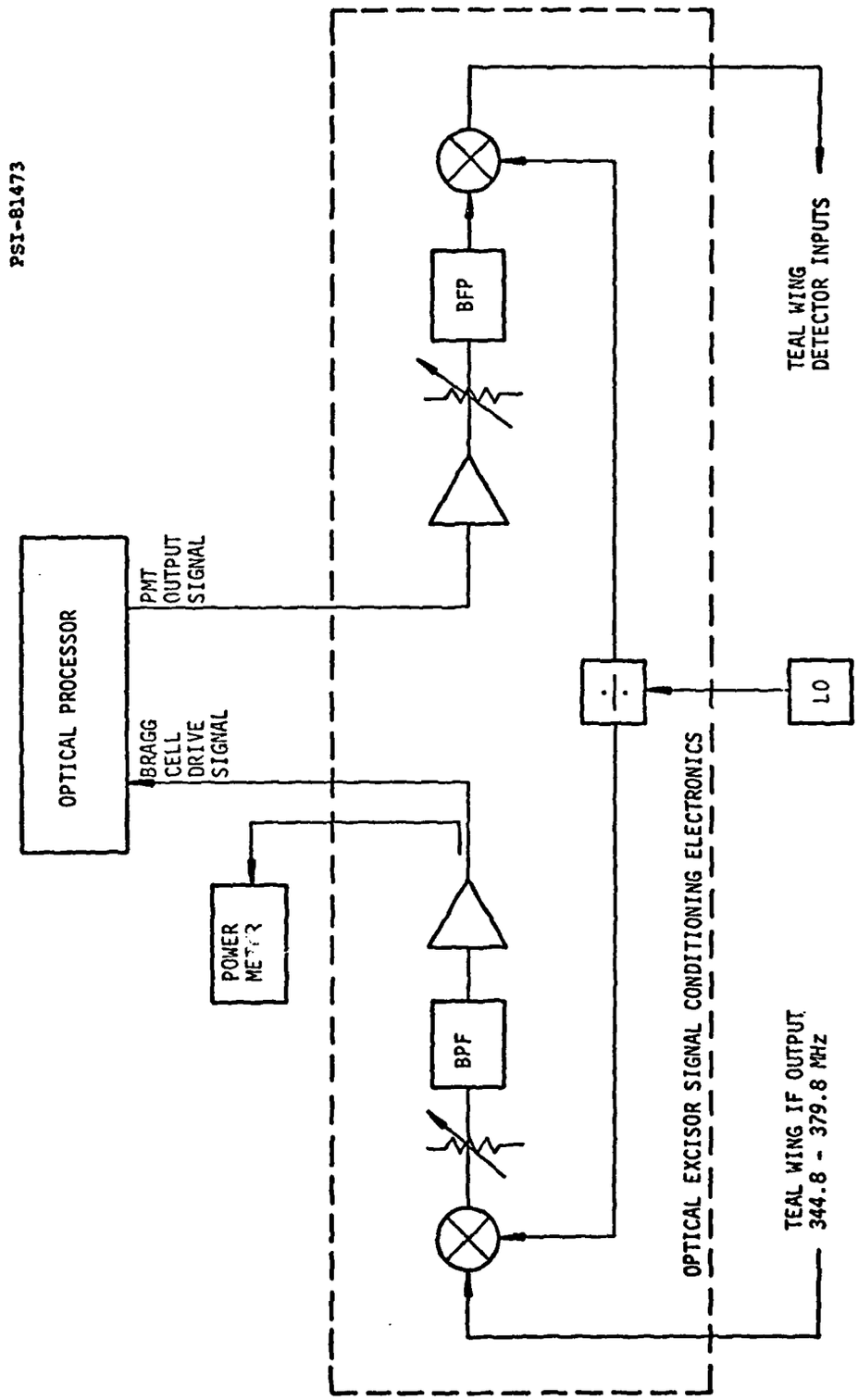

FIGURE A-2 EXCISOR ELECTRONICS BLOCK DIAGRAM

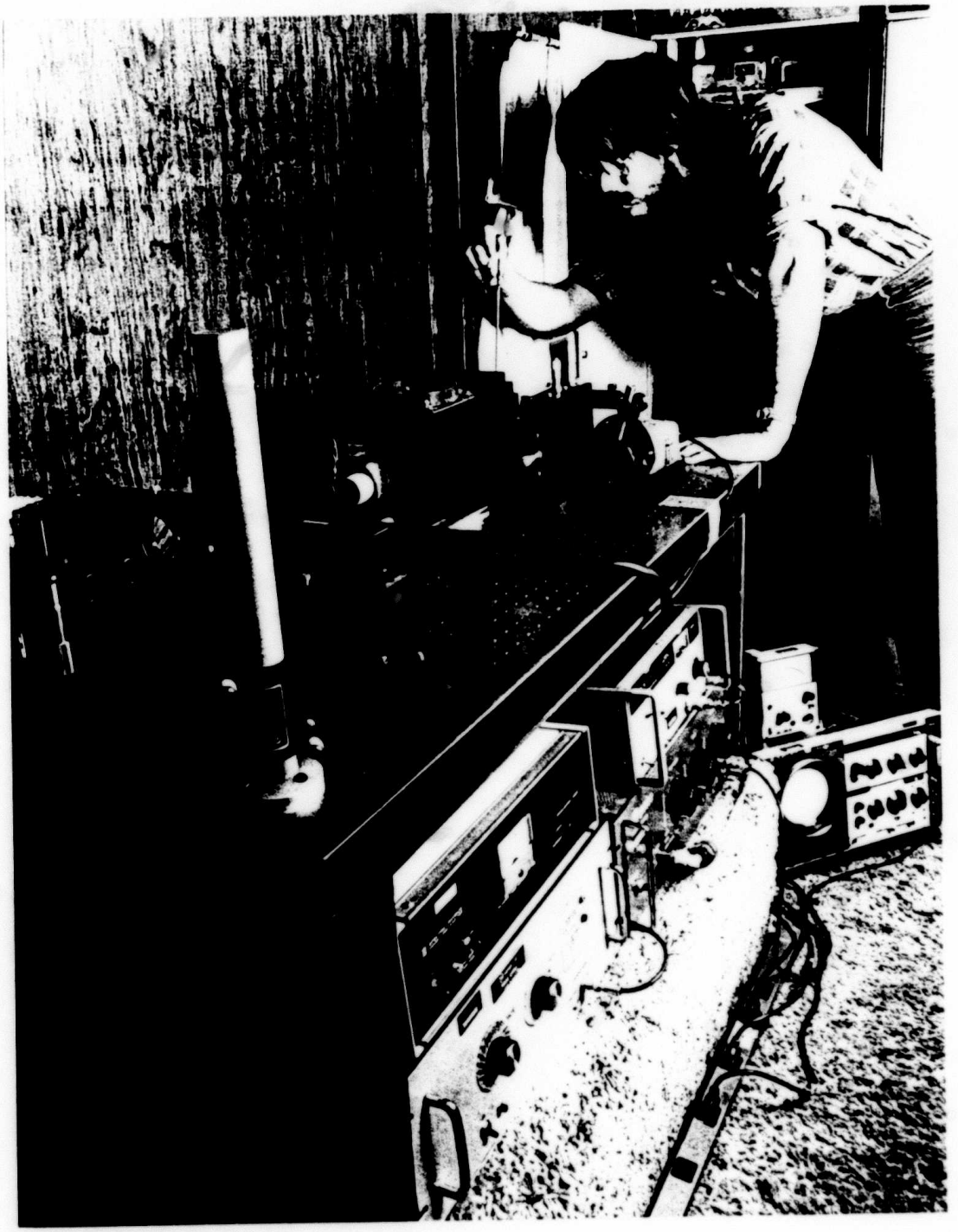

FIGURE A-3

PHOTO OF BRASSBOARD OPTICAL SIGNAL EXCISOR

APPENDIX B
INTRODUCTION

This appendix describes the capabilities of the equipment that was used in measurements of the optical excisor. Such measurements ensured that the performance of the excisor is adequate for eliminating interference signals in a spread spectrum intercept system.

B.1 EXISTING TEAL WING SYSTEM DESCRIPTION

The block diagram in Figure B-1 and the table of system specifications, Table B-1, detail the system hardware organization and general performance. The two IF channels distribute the signals to the various radiometers and feature detectors. For the optical excisor experiments, the chip detector and the switched radiometer were used with the IF frequency centered at 362 megahertz.

B.2 TEST EQUIPMENT DESCRIPTION

As shown in Figure B-2 the intercept system is divided into two equipment groups; a receiving interface and a basic intercept group. The interface is used to adapt to different intercept scenarios such as back-to-back tests, field tests, changes in RF frequency band or airborne testing utilizing existing aircraft antennas, etc. The basic intercept system provides the processing, detection, and recording necessary for intercept operation.

B.2.1 Basic Intercept System Description

Figure B-3 is a simplified block diagram that shows that the basic intercept system consists of four sections: (1) a dual-channel IF processor, (2) the signal detectors, (3) the recording system, and (4) the test subsystem.

For ease of operation and portability the basic intercept system hardware is mounted in three standard 19" width racks and normally mounted in a

TABLE B-1 SYSTEM SPECIFICATIONS

OVERALL	
Receiver Phase Match	±15° (1 dB IF BW)
Gain Match	±1 dB
RECEIVER	
Noise Figure	3.3 dB
RF Coverage	260-460 MHz
IF Bandwidths	10 MHz, 20 MHz, 35 MHz, 100 MHz, 120 MHz, 200 MHz
PROCESSORS	
Correlation Radiometer	
Detection Performance	Square Law
Maximum TW Product	4×10^{10} or 106 dB (200 sec T, 100 MHz BW)
IF Bandwidths	10, 20, 35, 120, 200 MHz
Integration TC	0.1-100 sec
Switched Radiometer	
Detection Performance	Square Law
Maximum TW Product	4×10^{10}
IF Bandwidths	10, 20, 35, 100, 120, 200 MHz
Integration TC	0.1-100 sec
Switch Rate	100 Hz
RF Switch	Ferrite
AC Radiometer	
Detection Performance	Fourth Law
Maximum TW Product	1.6×10^{9} or 92 dB (50 MHz IF, LPF 0.2 Hz, 200 sec T)
IF Bandwidths	50/50 MHz
Integration TC	1-100 sec
Chip Detector	
Detector Performance	Square Law
Maximum TW Product	2.5×10^{9} (200 MHz IF, Equiv T = 12.5) or 94 dB
IF Bandwidths	10, 20, 35, 100, 120, 200 MHz
Minimum Analyzer BW	0.16 Hz
Selectable Delay	6, 12, 25, 50, 100 nanoseconds and all combinations
Chip Frequency Range	0.2-100 MHz

TABLE B-1 (Continued)

PROCESSORS (continued)

Doubler

Detector Performance	Square Law
Maximum TW Product	2.5×10^9
IF Bandwidth	10, 20, 35, 50, 100, 120, 200 MHz
Minimum Analyzer Bandwidth	0.16 Hz

Hop Rate Detector

Detector Performance	Fourth Law
Maximum TW Product	2.5×10^8 or 84 dB
IF Bandwidths	50/50 MHz
Minimum Analyzer BW	0.16 Hz
Hop Rate Range	0.3-500 Hz; 3000 Hz with mod.

ANALYSIS EQUIPMENT

Real Time Spectrum Analyzer

Spectral Dynamics SD330 Spectrascope

Frequency Range	0.15 Hz-20 kHz in 9 ranges
Dynamic Range	48 dB
Noise Level	54 dB
No. of Frequency Cells	250
Resolution	0.15 Hz
Averaging	Simple Average 1 - 512 Peak Hold 1 - ∞ Exponential Average 1 - ∞

Frequency Translator

Spectral Dynamics SD332 Spectrum Translator

Input Frequency Range	10 Hz-150 kHz
Translated Frequency	0-25 Hz
(Plug-in Cards)	0-100 Hz, 0-1 kHz, 0-20 kHz

Strip Chart Recorder

Hewlett Packard 7100 Dual Channel, Overlapping Pen Coverage

Chart Size	10 inches
Chart Speed	2 in./sec - 1 in./hr (12 steps)
Voltage Span	1 mV - 100 V FS (16 steps)
Pen Type	Ink or Electric Writing

TABLE B-1 (Continued)

ANALYSIS EQUIPMENT (continued)

X-Y Plotter

Hewlett Packard 7035BR	
Chart Size	8-1/2" x 11"
Pen Lift	Local and Remote
Chart Hold Down	Electrostatic

RF Spectrum Analyzer

HP8558B	
Frequency Coverage	0.1-1500 MHz
Bandwidth	1 kHz to 3 MHz (8 steps)
Frequency Accuracy	<±5% of Indicated Separation

TEST EQUIPMENT

VHF Signal Generator

Hewlett Packard 608 ER	
Range	10-480 MHz (5 bands)
Accuracy	0.5%
Drift	50×10^{-6}/10 min

Power Meter

HP432A	
Frequency Range	10 MHz to 10 GHz
Accuracy	±1% (<±0.1 dB)
Pacific Meas. Type 1009	
Frequency Range	10 MHz to 12.4 GHz
Accuracy	±0.3 dB
Linearity	<0.4 dB for 50 dB change

Attenuators

HP355C Variable (calibrated)	
Frequency Range	dc to 1000 MHz
Atten. Range	0 to 12 dB
Atten. Accuracy	<0.25 dB, dc to 500 MHz
Residual Atten.	<0.5 dB
Calibration Accuracy	<0.1 dB
HP355D Variable (calibrated)	
Frequency Range	dc to 1000 MHz
Atten. Range	0 to 120 dB
Atten. Accuracy	0 to 90 dB ±1.5 dB
	90 to 120 dB ±3 dB
Residual Atten.	<0.5 dB
Calibration Accuracy	<0.3 dB to 40 dB
	<0.5 dB to 70 dB

TABLE B-1 (Continued)

TEST EQUIPMENT (continued)

Attenuators (continued)

HP8491 Fixed (calibrated)

Frequency Range	dc to 12.4 GHz
Atten. Accuracy	±0.5 dB
Calibration Accuracy	±0.1 dB

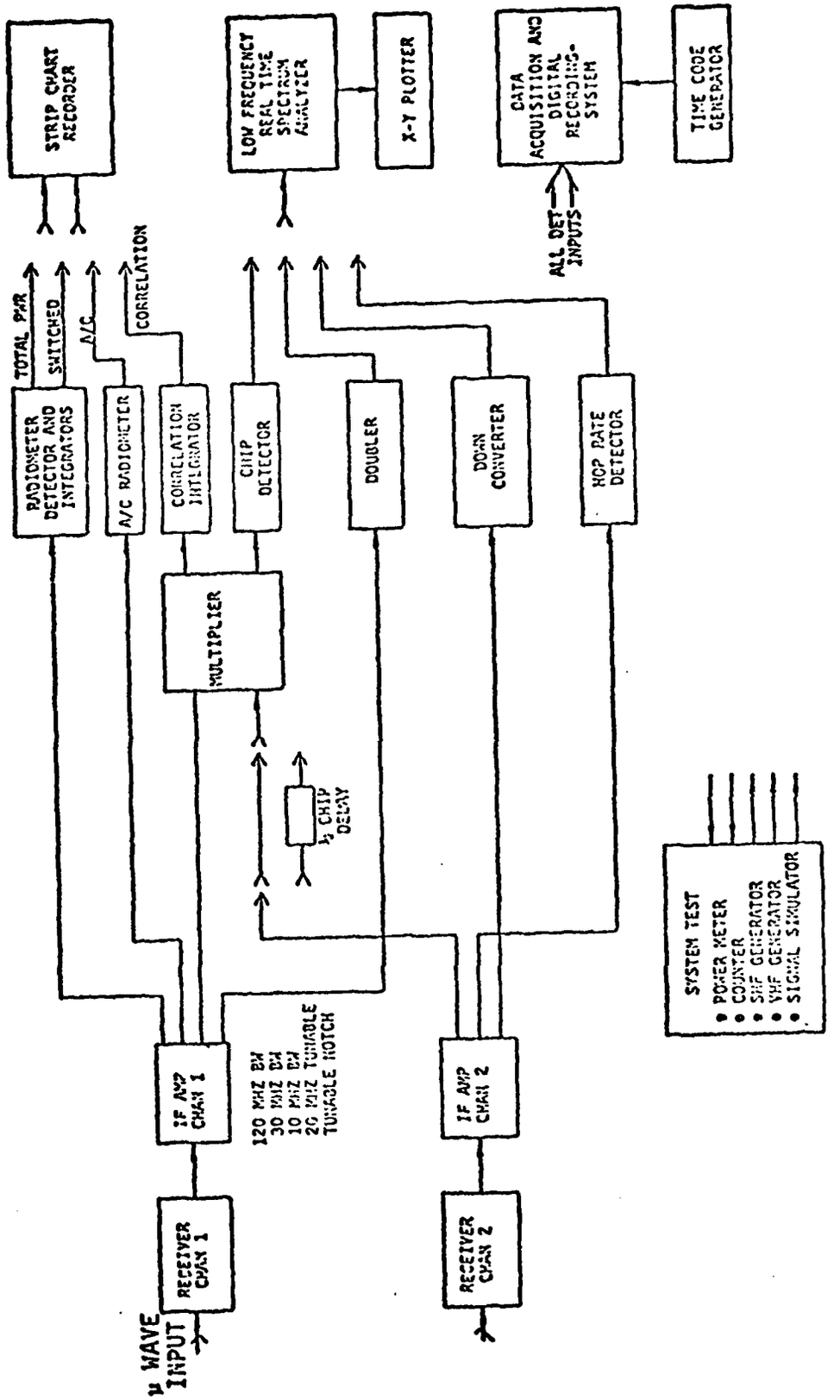

FIGURE B-1 TEAL WING INTERCEPT SYSTEM CONFIGURATION

0122A

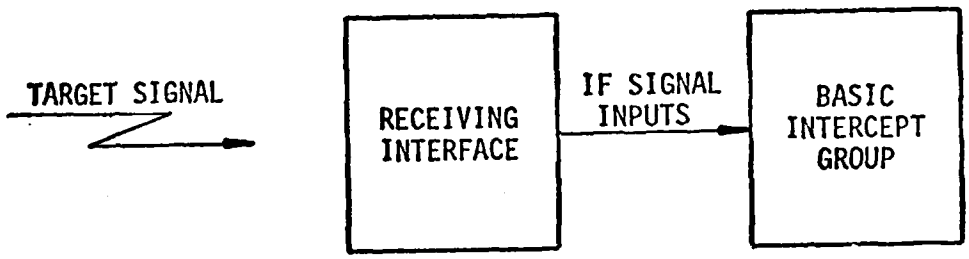

FIGURE B-2 INTERCEPT SYSTEM

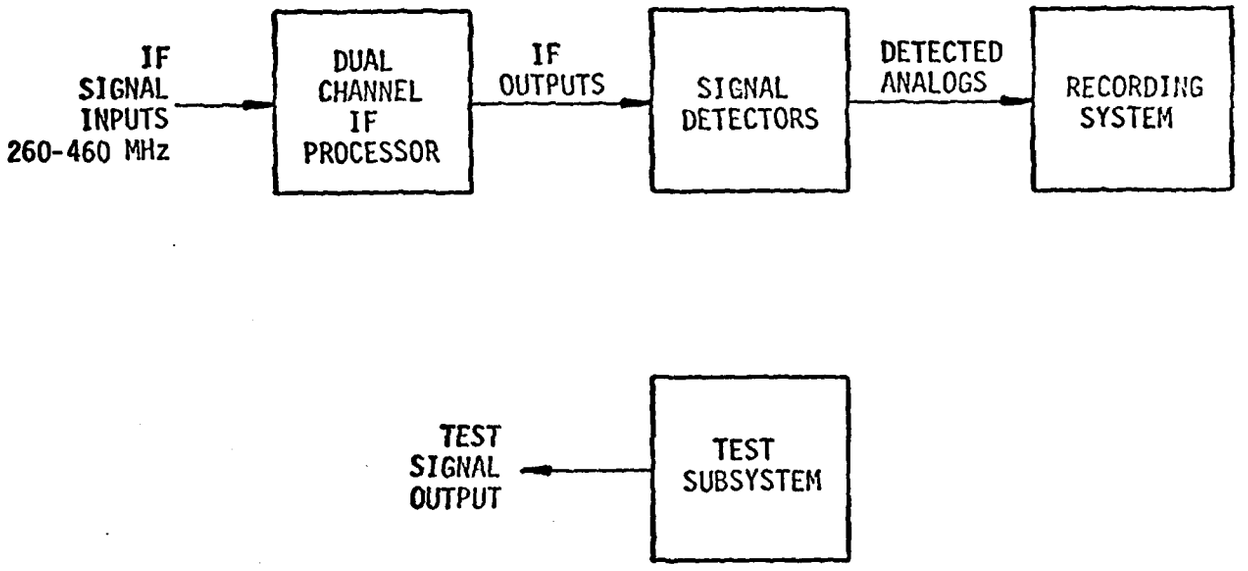

FIGURE B-3 BASIC INTERCEPT GROUP

van. The equipment is grouped so that one or two seated operators can easily operate all of the required equipment.

The IF Processor (shown in Figure B-4) consists of two amplitude and phase matched channels, each with wide and narrowband fixed and tunable bandpass preselect filters as well as notch filters for strong interference rejection. All preselect filters are available for patching into the system to provide the maximum intercept bandwidth that the environment will allow. Both IF channels are required for the correlation radiometer and delay chip detector. Only one IF is utilized for the other detectors. For the switch radiometer the RF switch is inserted in IF2 before the preamplifier. The system noise figure is set by a low noise preamplifier inserted after the preselect filters. The output of the preamplifier is fed to a high gain IF filter-amplifier circuit. The IF filters are multipole patch-in units to increase processing flexibility. The IF output is power divided and fed to the signal detectors.

The heart of the intercept system consists of seven separate signal detectors (see Figure B-5). Four radiometers, a square law doubler, a chip rate detector and frequency hop detector are incorporated. An audio detector is also available for monitoring interfering signals.

The four radiometers were incorporated in order to evaluate the comparative performance of each. The gain stability required for large time-bandwidth (TW) products makes use of the total power radiometer very ineffective and required use of a gain-stabilized switched radiometer. The switched or Dicke radiometer was the one used in this set of field tests. Its output was recorded on one channel of a dual channel strip chart recorder. The recorded output is the receiver input power versus time integrated over the IF bandwidth and radiometer time constant. The correlation radiometer illustrates the advantages to be gained by processing only the correlated component of two independent receiver channels. The AC radiometer provides a detector with high immunity to fixed interference and radiometer performance.

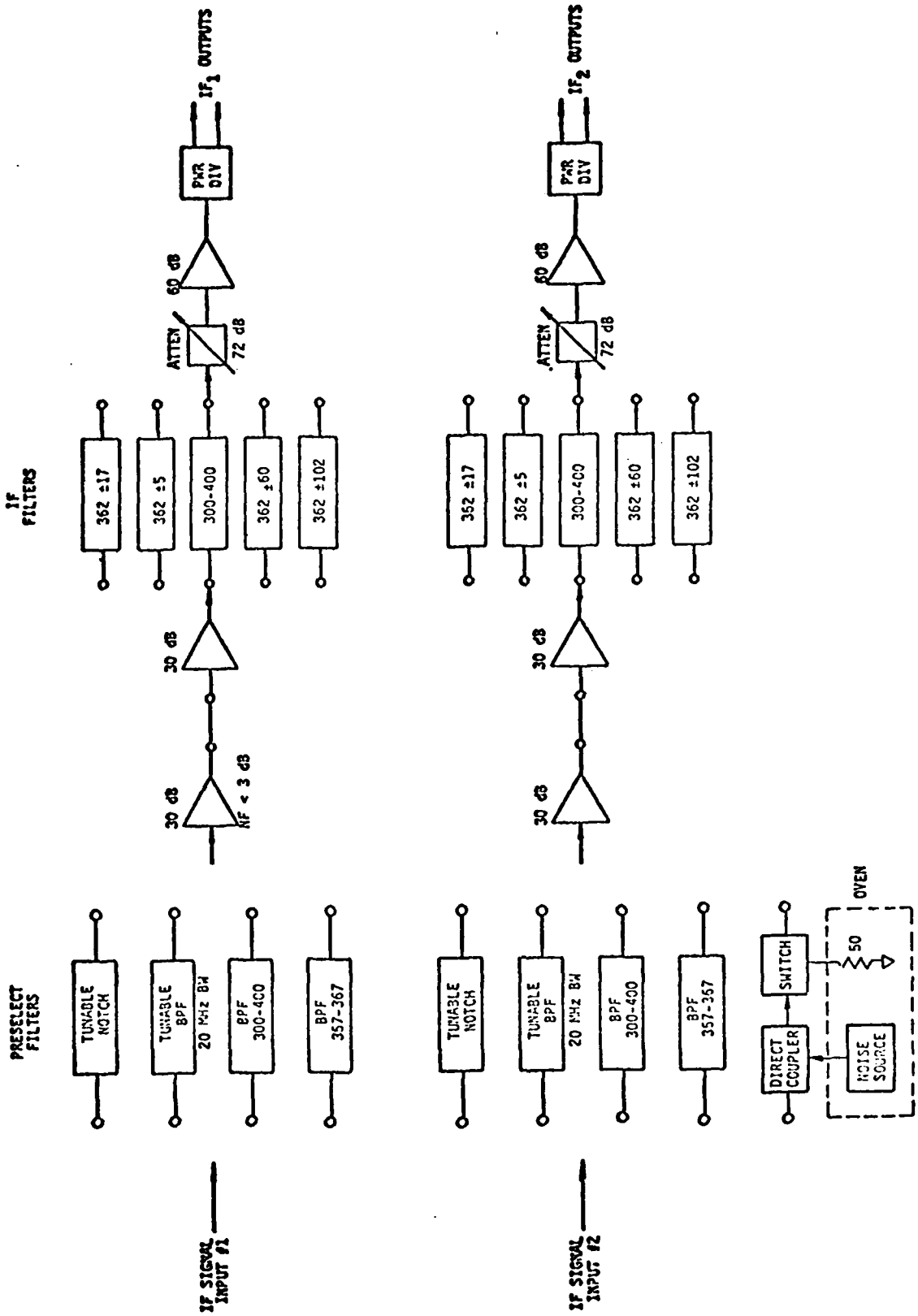

FIGURE B-4 DUAL CHANNEL IF PROCESSOR

0122A

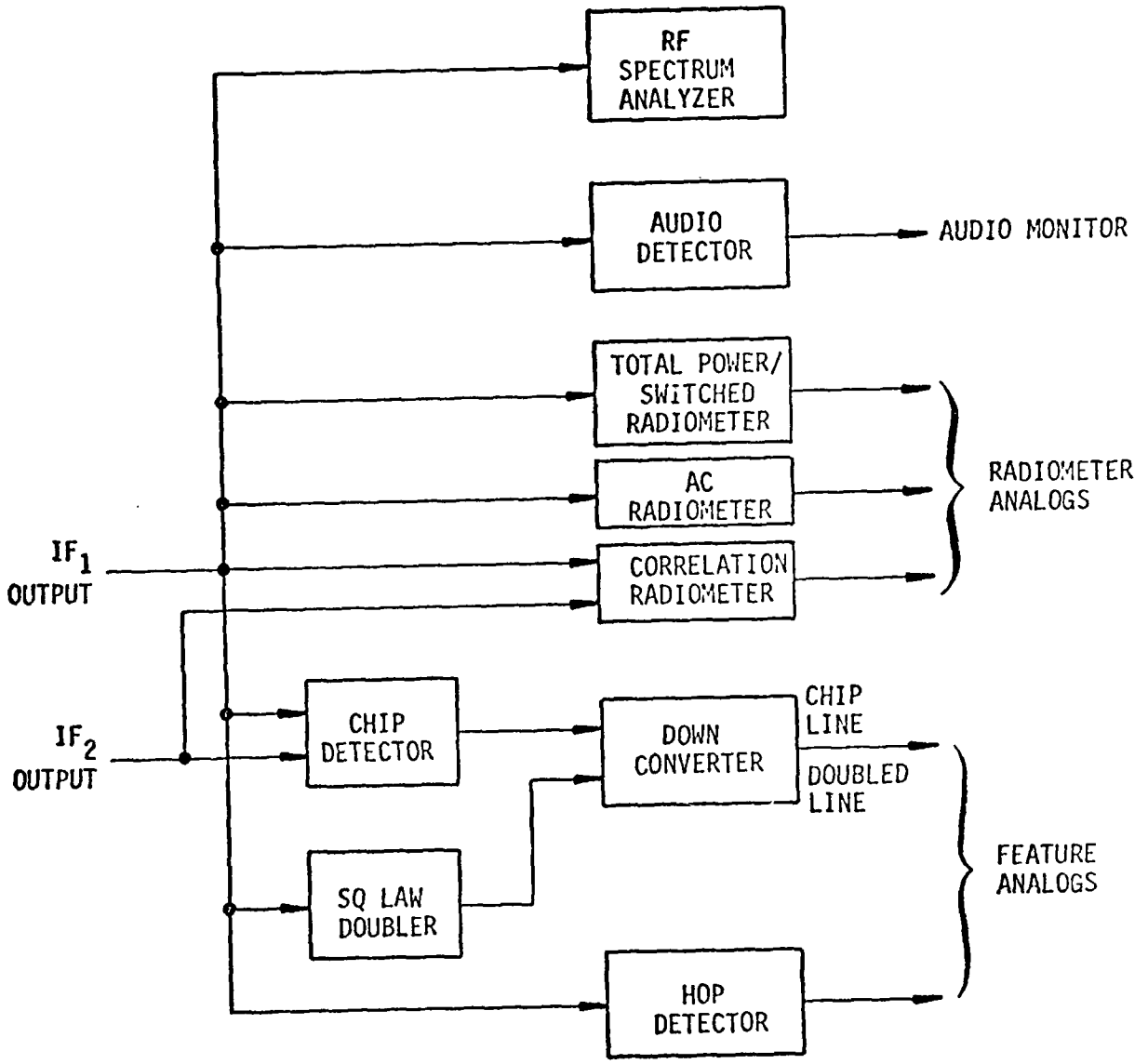

FIGURE B-5 SIGNAL DETECTORS

The doubler is used to collapse biphase and quadrature phase modulated PSK to a single spectral line. The collapsed line or lines can be processed with a very narrow bandwidth to achieve a large TW product.

The chip rate detector is used to detect the spreading or chip rate if the PN sequence. Two techniques are utilized; simple square law detection to detect filter-induced signal AM and signal delayed by 1/2 the chip rate and multiplied to give an output pulse at each bit transition. The spectral line at the chip rate is viewed with a narrow bandwidth for a large TW product. The latter technique was used in this report and the spectral line at the chip rate was detected on a real time spectrum analyzer averaged and then recorded on either the X-Y recorder or a photo of the spectrum analyzer scope.

The hop detector detects the rate at which the signal frequency hops and it can also be used to detect the rate inherent in the time hop pulse duration. Two techniques are available; simple square law detection as the second detector to detect filter-induced signal AM and signal delayed by 1/2 the hop rate or for time hopping 1/2 the pulse duration and multiplied to give an output pulse at each bit transition. The fourth law detected spectral line is viewed with a narrow bandwidth for a large TW product.

The audio detector and RF spectrum analyzer provide a means of detecting interfering signals. The dc analogs produced by the radiometers and the spectral lines generated by the feature detectors are fed to the recording subsystem (Figure B-6) to be displayed and recorded for data analysis.

The recording subsystem consists of dual audio speakers, a dual channel strip chart recorder, a realtime deltic spectrum analyzer and X-Y chart recorder. The radiometer outputs are patched to a dual channel strip chart recorder for continuous monitoring. The strip chart provides a hard copy record illustrating noise characteristics, dc drift, interference and signal processed output SNR. The realtime spectrum analyzer with 0.15 Hz bandwidth is utilized for all narrow spectral line analysis. The doubled carrier line and chip rate line are down converted for display on this analyzer. The hop and time hop feature lines are translated within the spectrum analyzer for display. The

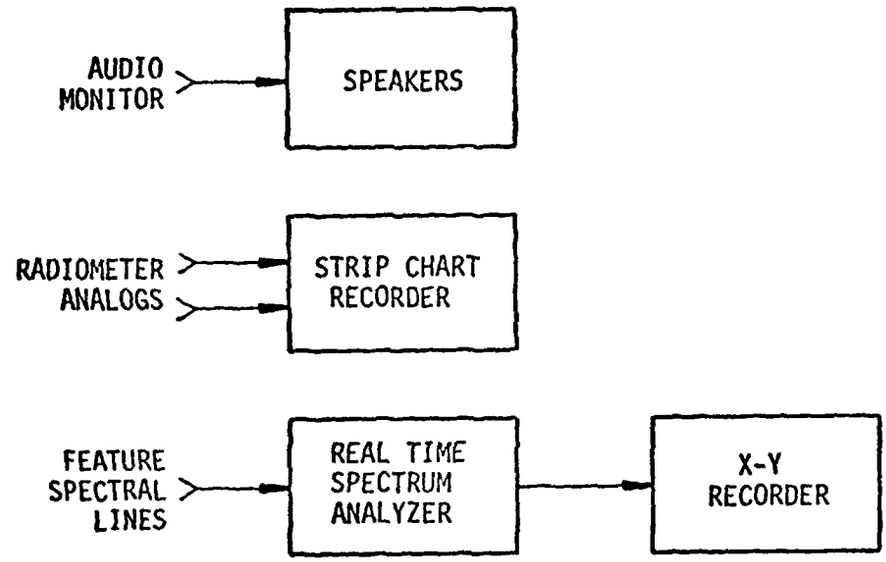

FIGURE B-6 RECORDING SYSTEM

0.15 Hz bandwidth (0.162 Hz noise bandwidth) achieves a time-bandwidth product similar to a 6-second radiometer time constant. The spectrum analyzer output can be recorded on an X-Y plotter for hard copy.

The test subsystem (Figure B-7) provides a means of system checkout and calibration and waveform evaluation. An RF signal generator or an HP synthesizer are used in various test modes to provide the chip clock or the CW carrier for spreading by the test signal generator (TSG). The test generator utilizes programmable PN generators to provide a PN spread signal for system performance analysis. A detailed description of the TSG is given later. A digital readout power meter aids in setting system power levels and in system calibration. The frequency counter is used for monitoring the test generator, bandpass calibration, and spectrum evaluation. Specifications for the equipment utilized in the intercept system are given in Table B-1. Nomenclature and general specifications for all commercial equipment used in the system is also given in Table B-1.

The TSG used to simulate the waveforms for detector test and evaluation is an LPI signal generator built on Teal Wing but modified to expand the frequency hop (FH) capability and provide time hop (TH) hybrid signals. All major single, double or triple hybrid waveform types with or without burst can be generated for a total of 32 different waveform types. The waveform variations are given in Table B-2. In addition to the waveform variation the modulation clock rate and parameters are selectable. The chip PN clock is internally selectable from 50 kHz to 40 MHz. Frequency hop rates and time hop frame rates are selectable from 1 to 1000 Hz. All of the clocks may also be externally controlled. The FH center frequency may be adjusted from 1 to 499 MHz and the hop bandwidth chosen from 0 to 200 MHz both in 1 MHz increments. A nonfrequency hopping (NFH) waveform can be selected in two ways: (1) the hop bandwidth can be set to 0 or 2) the synthesizer providing the carrier frequency can be switched from remote to local control and the desired carrier frequency set into the synthesizer directly. The time hop (TH) pulse duty cycle may be selected with 1/8, 1/16, or 1/32 duty factor available. A burst signal can be generated by selecting external gate control and supplying a TTL compatible control signal to the gate input. Burst signals of single pulse or repetitive

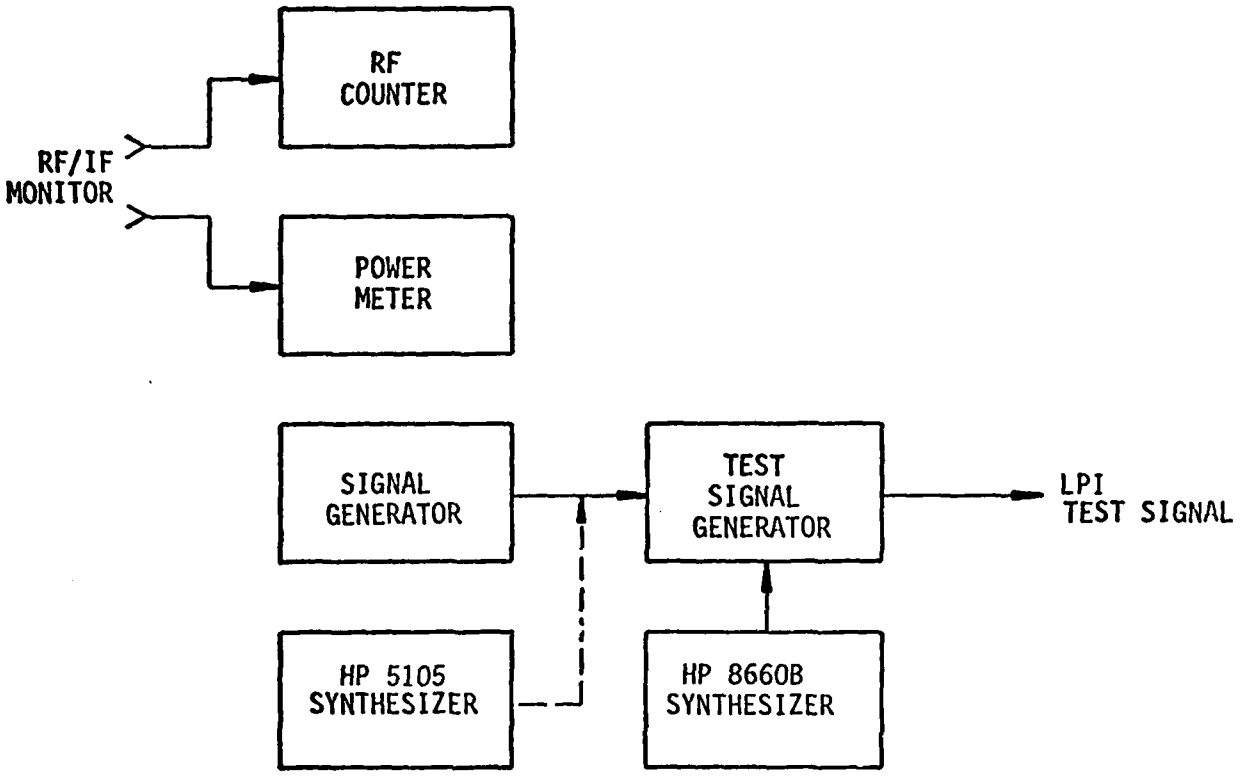

FIGURE B-7 TEST SUBSYSTEM

TABLE B-2 TSG HYBRID VARIATIONS

PHASE MODULATION	FREQUENCY HOPPING	TIME HOPPING	BURST
CW	NFH	NTH	Continuous
BPSK	FH	TH	Burst
QPSK			
SQPSK			

bursts with pulse durations from 100 μsec to continuous transmission can be accepted.

A block diagram of the TSG is shown in Figure B-8. The only interface required is with an HP-5105 synthesizer. The synthesizer provides the carrier frequency for the TSG and a 20 MHz reference input to the internal clock that provides the chip frequency and time hop rates. The synthesized carrier frequency is controlled by the TSG. Frequency hopping is accomplished by hopping the carrier within the synthesizer. The carrier frequency passes through a modulator that is controlled by the time hop/burst generator. The time hop generator also controls the PN generators to increase the isolation during the "off" time. The output from the time hop modulator passes through a 90° hybrid to give the quadrature carriers required for QPSK and SQPSK waveform generation. The quadrature carrier passes through two modulators controlled by two 12-stage LSG PN generators. When PN-"OFF" (CW) is selected both PN generators are disabled, the inphase modulator is turned fully on and the quadrature modulator turned off. For BPSK the quadrature modulator is still off but the BPSK PN generator is enabled. QPSK is generated by enabling both PN generators and modulators and adding the modulator outputs in a 180° hybrid. Because both modulators are enabled in QPSK the output signal level is 3 dB higher than CW or BPSK. SQPSK is generated the same as QPSK except that the

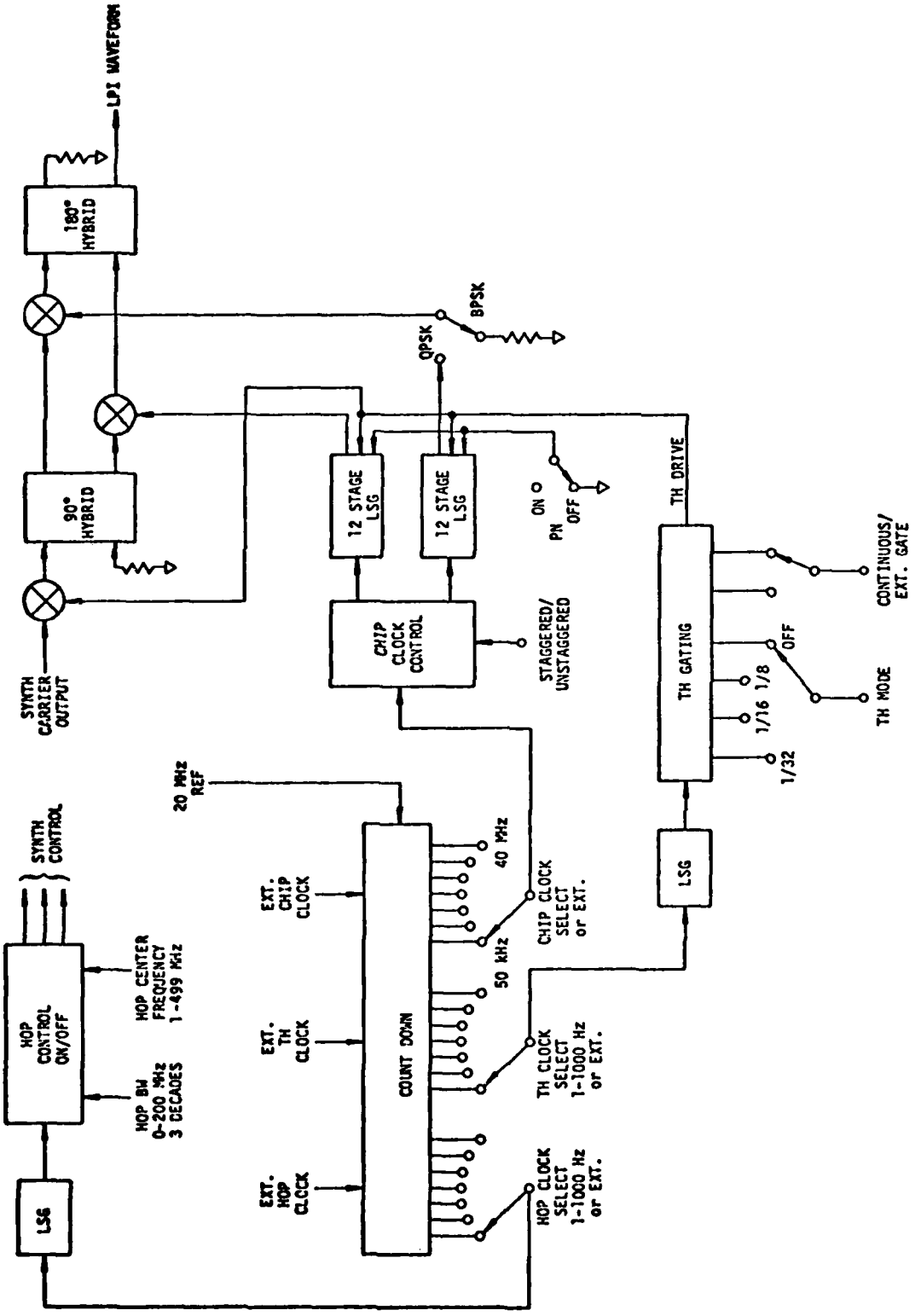

FIGURE B-8 TEST SIGNAL GENERATOR BLOCK DIAGRAM

clocks for the PN generators are staggered within the chip clock control unit. By building the TSG as a series of independent stages an extremely versatile LPI simulator can be built at a modest cost. The primary limitation of this approach is that when operating in any PN/FH mode that the PN waveform cannot be filtered prior to frequency hopping.

APPENDIX C
EXCISION REQUIREMENTS FOR SPREAD SPECTRUM INTERCEPT

C.1 EXCISION REQUIREMENTS

The requirement for excision in any given intercept system is dependent on the type of detectors and signal levels involved. It is also heavily influenced by the required frequency band of operations. For example, the HF band presents an extremely crowded environment of interfering signals *and* a time-varying noise background. At these frequencies, the probability of obtaining interference-free intercept, over any significant frequency band, is quite low. At UHF frequencies, the signal environment can also be quite dense. In these cases, there is often considerable performance improvement possible with excision techniques. In less crowded signal environments, successful intercept operations may be feasible without excision, or with a minimal excision capability.

The signal environment also influences the type of excision capability required. With few interfering signals, a fixed excision function, such as provided by a few notch filters, may suffice. However, in a more crowded and highly dynamic signal environment, such as the HF band, a more flexible and time-varying excision capability is clearly required.

The requirement on any technique utilized for interference excision is the removal of as much of the interference-related energy as possible so that the spectrum that is input to the detectors is as interference free as possible. In excising the interference, it is desirable to remove as little of the desired signal(s) as possible. The following paragraphs present methods for evaluating the sensitivity degradation expected and the filter resolution required for an effective frequency excision process.

C.1.1 Signal, Interference, and Noise

For a straightforward analysis, we assume only one interfering signal,

$$i(t) = P \cos \omega_0 t$$

and one desired signal,

$$s(t) = a(t) \cos \omega_1 t \qquad a(t) = \pm A.$$

Define :

$$I = \frac{P^2}{2}, \text{ the interference power}$$

$$S = \frac{A^2}{2}, \text{ the signal power}$$

$$N = 2N_o W, \text{ the input noise power} .$$

The situation of interest is with S<<N, S<<I, but N≈I. The power density spectrum is shown in Figure C-1.

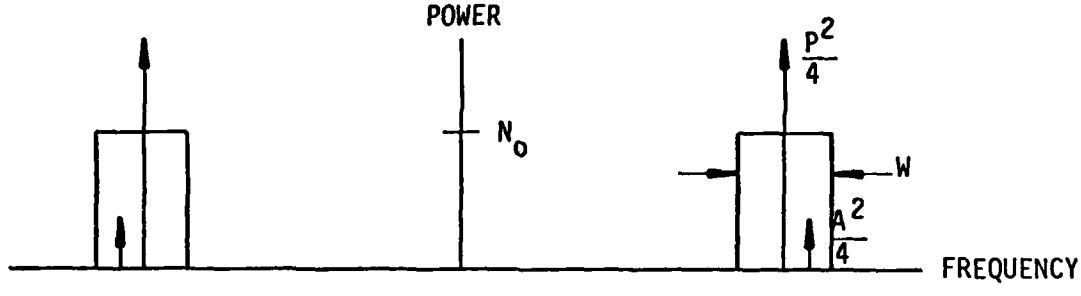

FIGURE C-1 INPUT SIGNAL SPECTRUM

After squaring and lowpass filtering, the spectrum centered at zero Hz is shown in Figure 4-2. Using a radiometer of lowpass bandwidth B, the output signal power, S_{out}, is $A^4/4 = S^2$. Also, referring to Figure C-2, the output noise power is

$$N_{out} = 2B\ (P^2N_o + 2A^2N_o + 4N_o{}^2W)$$

$$\approx \frac{4BNI}{W} + \frac{2BN^2}{W} \quad .$$

Thus

$$\left(\frac{S}{N}\right)_o = \frac{1}{2}\ \left(\frac{S}{N}\right)_i^2\ \ \frac{W}{B(1 + \frac{2I}{N})}$$

where

$$D = \frac{1}{1 + \frac{2I}{N}}$$

is the degradation in output signal-to-noise ratio caused by the interference. For example, a 5 dB degradation is caused when I/N = 1. This interference-induced sensitivity loss is plotted in Figure C-3. Until $I/N \geq 1$, the loss is not unreasonable.

Also, at $I/N \geq 1$ only a few excision filters are required to detect and remove the interference. For example, ten filters would yield a 10 dB output SNR for the filter containing the interference. This is easy to detect and remove. This same degradation applies to all square-law detectors such as doublers and chip rate detectors.

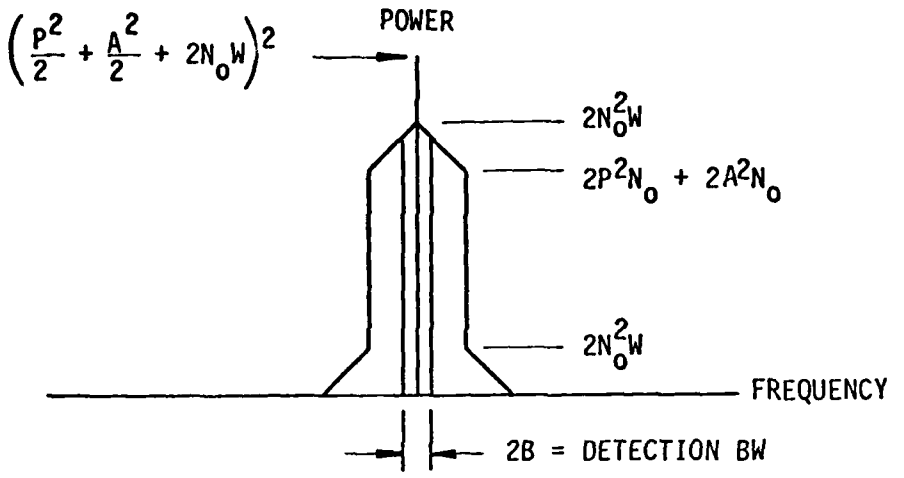

FIGURE C-2 SPECTRUM AFTER SQUARING

If the interference is weak (below the noise), it can still cause false alarms unless excised. For narrowband interference, excision is still possible if the filter resolution is fine enough. The required resolution or number of required filters is derived in the following section.

C.1.2 *Minimum Filter Resolution*

Since reliable radiometer detection is achieved at

$$\left(\frac{S}{N}\right)_o = 10 = \left(\frac{S}{N}\right)_i^2 TW ,$$

the minimum detectable signal power, S_{min}, is

$$S_{min} = N_oW \left(\frac{10}{TW}\right)^{\frac{1}{2}} .$$

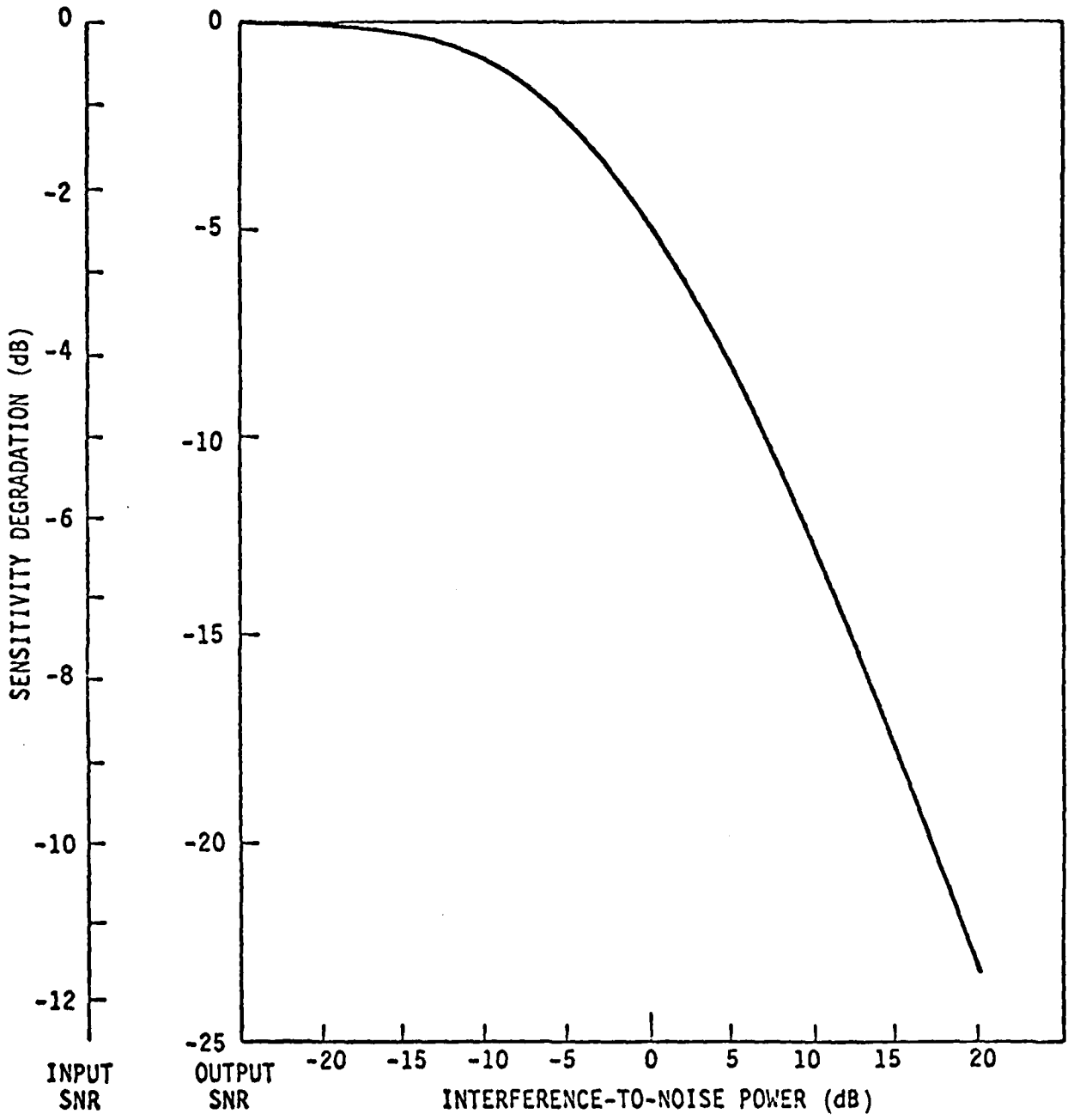

FIGURE C-3 SENSITIVITY DEGRADATION CAUSED BY INTERFERENCE

Any interfering signal of power $I \geq S_{min}/2$ causes confusion, and $I \geq S_{min}$ causes a false alarm. If the interference is sufficiently narrowband compared to W, then linear detection (by means of spectrum analysis) and interference excision with filters of bandwidth W_E where $nW_E = W$ is possible. The interference is detectable when it is above the noise in a filter of bandwidth W_E; thus,

$$I \geq N_o W_E = \frac{N_o W}{n} .$$

To prevent false alarms, the undetected interference must be less than S_{min}. Hence,

$$\frac{N_o W}{n} \leq I \leq S_{min} = N_o W \left(\frac{10}{TW}\right)^{1/2}$$

and

$$n \geq \left(\frac{TW}{10}\right)^{1/2}$$

filters are required in the excision processing.

For example, at HF, a typical spread spectrum bandwidth may be 100 kHz and 10 s

$$n \geq \sqrt{\frac{10^6}{10}} \cong 316$$

filters would be required. The only reasonable way to realize this number of filters is with the fast Fourier transform (FFT). With an FFT used to implement n filters, about 6 times finer resolution is required to account for notch width

or passband shaping. Thus, a 2000 point complex transform could implement 300 filters for good interference excision and eliminate all narrowband interference at power level $\geq S_{min}$.

C.2 EXCISION IMPLEMENTATION

To maximize spread spectrum intercept system sensitivity and minimize the effect of the degradations discussed previously, it is desirable to implement a method of excising interfering signals from the spectrum that is input to the detectors. The closer the excision process can come to creating an interference-free Gaussian noise environment, the closer the resulting detector performance will be to theoretical.

C.2.1 Frequency Excision

(U) Frequency excision is generally more complex than time excision. The range of available frequency excision techniques is quite broad, extending from the relative simplicity of a tunable notch filter to the hardware complexity (and cost) of large analog filter banks. Digital implementations of a filter bank are also feasible in some applications. In the paragraphs that follow, we will discuss the tradeoffs pertinent to selecting from the wide range of frequency excision approaches.

The successful approach must have a strong function of the nature of the interference environment in which the intercept system must operate. In the case of a relatively clean environment with few interfering signals, the use of a few tunable notch filters can provide an effective and relatively simple low-cost excision approach. On the other hand, a large number of interfering signals, or a highly dynamic interference environment, or both, may require the use of a bank of contiguous filters.